Supporting Information

Tuning the Structure of N- methyldiethanolamine-based Deep Eutectic Solvents for Efficient and Reversible SO_2 Capture

Xueqi Li[a], Lingqiang Meng[a], Fuliu Yang[a], Zhuhong Yang[a*], Jun Li[a], Yifeng Chen[a,b *], Xiaoyan Ji[c]

[a]College of Chemical Engineering, Nanjing Tech University, Nanjing 211816, China

[b]Institute of Chemical Industry of Forest Products, CAF; National Engineering Laboratory for Biomass Chemical Utilization; Key and Open Laboratory of Forest Chemical Engineering, SFA; Key Laboratory of Biomass Energy and Material, Nanjing 210042, China

[c]Energy Engineering, Division of Energy Science, Luleå University of Technology, Luleå 97187, Sweden

E-mails: zhhyang@njtech.edu.cn

Chemicals

N_2 (>99.9%, vol%) and SO_2 (2%, vol%) were supplied by Nanjing Special Gas Factory. N-methyldiethanolamine (98 wt%), imidazole (99 wt%), 1,2,4-triazole (99 wt%), and tetrazole (98 wt%) were supplied by Shanghai Aladdin Reagent Co., Ltd. Sodium hydroxide (98 wt%) was obtained Sinopharm Chemical Reagent Co., Ltd.

Characterization

FT-IR spectroscopy were obtained with a Thermo Fisher Scientific Nicolet iS50 spectrometer in the range of 400-4000 cm^{-1}. A Bruker spectrometer (500 Hz) was used for the ^{1}H and ^{13}C NMR spectroscopy using DMSO as the solvent to confirm the structure of the DESs. The thermal stability of DESs was analyzed by a simultaneous thermal analyzer (NETZSCH STA 409PC) with a scan rate of 10 $K \cdot min^{-1}$ from 300 K to 800 K under N_2 atmosphere. The density of DESs was measured with a 25 mL specific gravity bottle with a measurement accuracy of 0.001 $g \cdot cm^{-3}$, where deionized boiling water was used as the calibration agent. The viscosity was measured by a rotary viscometer (NDJ-95) with an accuracy of ±5%. The melting points of DESs were determined using differential scanning calorimetry (NETZSCH DSC 200 F3). Under N_2 atmosphere, the sample was firstly cooled to −80 °C with a rate of 5 $°C \cdot min^{-1}$ to ensure complete crystallization. Then, the sample was heated to 30 °C with a rate of 10 $°C \cdot min^{-1}$ after isothermal for 0.5 h.

Computational Methods

The geometries of all species were optimized by using the Møller-Plesset perturbation method (MP2) with the Gaussian 09 program.[1] For all elements, the diffuse 6-31++G** basis set was applied. Frequency calculations were performed to determine the minimum and obtain the thermochemical properties of all species. Gibbs free energies were computed at 298.15 K and 1 atm. The enthalpy change during SO_2 binding is defined as the difference of enthalpy between the species after SO_2 binding and the absorbent and SO_2. For example, binding enthalpy change ($\Delta H_{B,1}$) = H(MDEA-Im+SO_2) − H(MDEA-Im) − H(SO_2), where H(MDEA-Im+SO_2) is the enthalpy of the species after SO_2 binding with MDEA-Im. All structural diagrams

were drawn using the VMD software.[2]

Capture and Regeneration Experiments

The diagram of the SO_2 capture apparatus used in this study is shown in Figure S1. In this study, 2.0 g DESs was added to a custom-made glass reactor (diameter 14 mm, height 100 mm) and a mixture of N_2 and SO_2 was passed into the reactor, and the sand core was used for bubbling capture, and the whole device was immersed in a water bath, Different partial pressures of SO_2 were obtained using rotameter regulation, and flue gas analyzer was used to detect the SO_2 concentration at the inlet and outlet, and the data were recorded by computer at regular intervals, and the reaction was considered to reach equilibrium when the SO_2 concentrations at the inlet and outlet remained the same for 1h. NaOH solution was used to capture SO_2 in the tail gas to avoid environmental pollution.

SO_2 regeneration experiments were performed by N_2 bubbling at 363.3 K for 3h. Owing to the large SO_2 concentration at the beginning of desorption, the detection range of the flue gas analyzer was much smaller than the SO_2 concentration. For this reason, we added 0.3% hydrogen peroxide solution and methyl red ethanol solution to the tail gas bottle and measured the SO_2 desorption in DESs by titration method at regular intervals.[3] The temperature of capture and desorption was controlled by the water bath.

The SO_2 capture capacity (2000 ppm) was calculated by the following Eq. (1):[3]

$$C = \frac{V \times Ar_{SO2}}{10^6 M V_m C_{DESs}} \int_{t_0}^{t} [C_{in} - \varphi(x)]dx \quad (1)$$

where V is the simulated flue gas flow rate ($L \cdot min^{-1}$), Ar_{SO_2} is the relative molecular mass of SO_2 ($g \cdot mol^{-1}$), C_{in} is the inlet concentration of SO_2 in the simulated flue gas (ppm), $\varphi(x)$ is a function of the SO_2 export concentration as a function of time, M is the mass of DESs (g), V_m is the molar volume of the gas ($L \cdot mol^{-1}$), C_{DESs} is the DESs concentration. Finally, the capture capacity C was obtained by calculation ($g \cdot g^{-1}$).

Thermodynamic Analysis

Using the thermodynamic model of reaction equilibrium Formulas[4-5] can be used to fit the Henry coefficient and reaction equilibrium constant of SO_2 absorption at different temperatures. In this study, Henry's constant (H) and reaction equilibrium constant (K) were used to describe the physical and chemical capture properties of SO_2 by DESs. The capture of SO_2 in MDEA-Im can be divided into the following two steps: 1) physical dissolution of SO_2 in MDEA-Im (Eq. (2)); 2) reaction of SO_2 with MDEA-Im in a 1:1 molar ratio (Eq. (3)):

$$SO_2\ (g) \rightarrow SO_2\ (l) \qquad \left(H_{SO_2}(T)\right) \tag{2}$$

$$SO_2\ (l) + DES\ (l) \rightarrow SO_2DES\ (l) \qquad \left(K_1\right) \tag{3}$$

The whole chemical capture reaction can be expressed by Eq. (4):

$$SO_2\ (g) + DES\ (l) \rightarrow SO_2DES\ (l) \qquad \left(K_2\right) \tag{4}$$

H, *K*, and Mass balance are expressed by Eqs. (5-8):

$$P = H_{SO_2}(T)\gamma_{SO_2(l)}\frac{m_{SO_2}}{m_0} \tag{5}$$

$$K_1 = \frac{\gamma_{SO_2DES}\dfrac{m_{SO_2DES}}{m_0}}{\gamma_{SO_2}\dfrac{m_{SO_2}}{m_0}\gamma_{DES}\dfrac{m_{DES}}{m_0}} \tag{6}$$

$$m_{DES,0} = m_{DES} + m_{SO_2DES} \tag{7}$$

$$m_{SO_2,t} = m_{SO_2(l)} + m_{SO_2DES} \tag{8}$$

where $m_{SO_2(l)}$ is the molar amount of free SO_2 (mol·kg^{-1}), m_{DES} is the molar amount of MDEA-Im (mol·kg^{-1}), m_{SO_2DES} is the molar amount of SO_2-MDEA-Im (mol·kg^{-1}), γ_{SO_2DES}、γ_{DES} and γ_{SO_2DES} represent the activity coefficients of each fraction in the liquid phase, m_0 is the standard weight (1 mol·kg^{-1}), $m_{DES,0}$ is the initial molar

amount of MDEA-Im in the liquid phase, $m_{SO_2,t}$ is the total solubility of SO_2 in MDEA-Im. The activity coefficients of all components in MDEA-Im are assumed to be uniform (γ=1), and Eqs. (5) to (8) are combined into Eq. (9):

$$m_{SO_2} = \frac{P}{H_{SO_2}(T)} + m_{DES,0}\frac{K_1 P}{K_1 P + H_{SO_2}(T)} \tag{9}$$

Based on the temperature-dependent values of $H_{SO_2}(T)$ and K_1, the desorption enthalpy (ΔH_{Des}) of SO_2 in MDEA-Im can be calculated using the following Eq. (10):

$$\Delta H_{Des} = \Delta H_{phy} + \Delta H_{chem} = -R\left(\left[\frac{\partial \ln H_{SO_2}(T)}{\partial(1/T)}\right] - \left[\frac{\partial \ln K_1}{\partial(1/T)}\right]\right) \tag{10}$$

where R is the gas constant (8.314 J·mol^{-1}·K^{-1}).

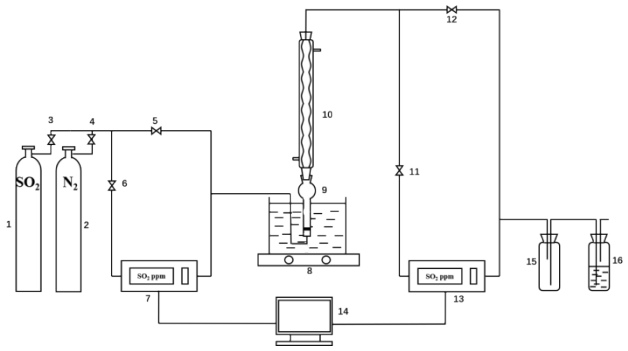

Figure S1. Schematic diagram of SO_2 capture and regeneration experimental setup:1-SO_2 cylinder; 2-N_2 cylinder; 3,4,5,6,11,12-valvers; 7,13-flue gas analyzer; 8-constant temperature water bath; 9-glass reactor; 10-condensate; 14-automatic data collection; 15,16-washing gas bottles.

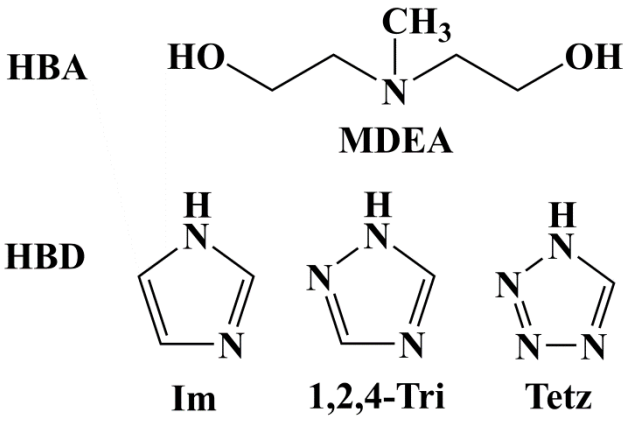

Scheme S1. Chemical structure of HBA and HBD.

Characterization and Physicochemical Properties of DESs

The structures of DESs were confirmed by nuclear magnetic resonance and Fourier transform spectroscopy, and the detailed results were shown in Figures S2-S6. Furthermore, the physicochemical properties were measured using a simultaneous thermal analyzer, densitometer, and viscometer. The results of thermal stability, density, viscosity and ionic conductivity were described in Figure S5, Table S1, Table S2 and Table S3, respectively. As shown in Figure S6, the melting points of all three mixtures were lower than −60 °C, while the melting point of MDEA is only −21 °C. Furthermore, Im, 1,2,4-Tri, and Tetz are solids at the room temperature, and their melting points are higher than −60 °C. Therefore, the mixtures in this study belong to DESs.

The ^{1}H NMR 、^{13}C NMR and FT-IR data of the as-prepared DESs.

MDEA-Im: ^{1}H NMR (500 MHz, DMSO-d_6) δ 7.76 (s, 1H), 7.08 (d, J = 1.5 Hz, 2H), 6.58 (s, 1H), 3.57 (t, J = 6.3 Hz, 4H), 2.52 (d, J = 6.4 Hz, 3H), 2.23 ppm (s, 3H);

^{13}C NMR (126 MHz, DMSO-d_6) δ 135.78, 122.09, 60.07, 59.12, 42.83 ppm;

FT-IR (4000-400 cm^{-1}) 3115, 2797, 1533, 1456, 1363, 1328, 1256, 1196, 1139, 1062, 1032, 929, 878, 820, 745, 661, 618, 475.

MDEA-1, 2, 4-Tri: ^{1}H NMR (500 MHz, DMSO-d_6) δ 8.28 (s, 2H), 6.89 (s, 1H), 3.48 (t, J = 6.2 Hz, 4H), 2.45 (t, J = 6.2 Hz, 4H), 2.20 ppm (s, 3H);

^{13}C NMR (126 MHz, DMSO-d_6) δ 147.28, 60.17, 59.21, 42.98;

FT-IR (4000-400 cm-1) 3113 2846 1459 1274 1151 1031 971 876 749 680 645.

MDEA-Tetz: ^{1}H NMR (500 MHz, DMSO-d_6) δ 8.46 (s, 1H), 6.44 (d, J = 5.7 Hz, 1H), 3.82 – 3.76 (m, 4H), 3.19 (t, J = 5.5 Hz, 4H), 2.80 ppm (s, 3H);

^{13}C NMR (126 MHz, DMSO-d_6) δ 148.46, 58.05, 56.15, 41.21 ppm;

FT-IR(4000-400 cm^{-1}) 3180, 2858, 1463, 1441, 1425, 1180, 1142, 1072, 998, 880, 699, 535, 434.

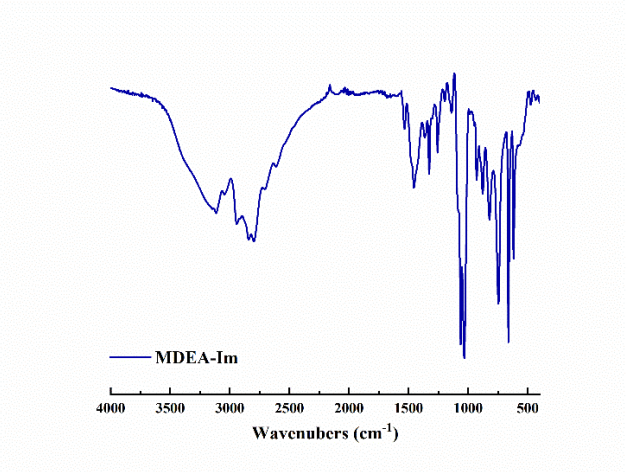

Figure S2. The FT-IR spectra of MDEA-Im.

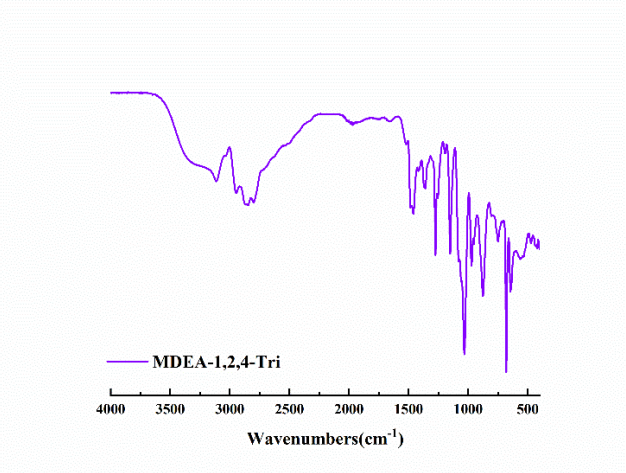

Figure S3. The FT-IR spectroscopy of MDEA-1,2,4-Tri.

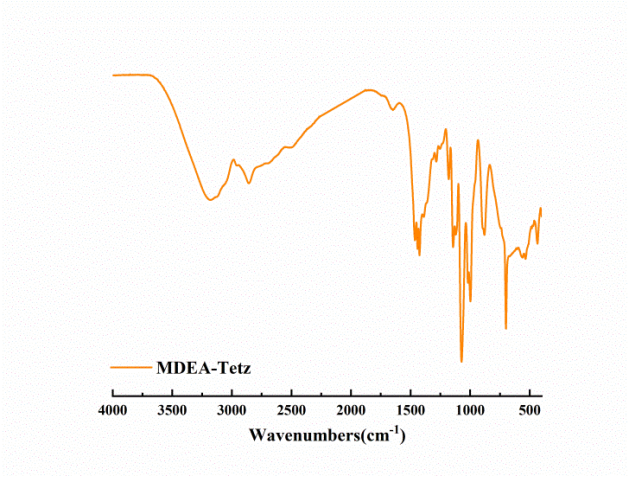

Figure S4. The FT-IR spectroscopy of MDEA-Tetz.

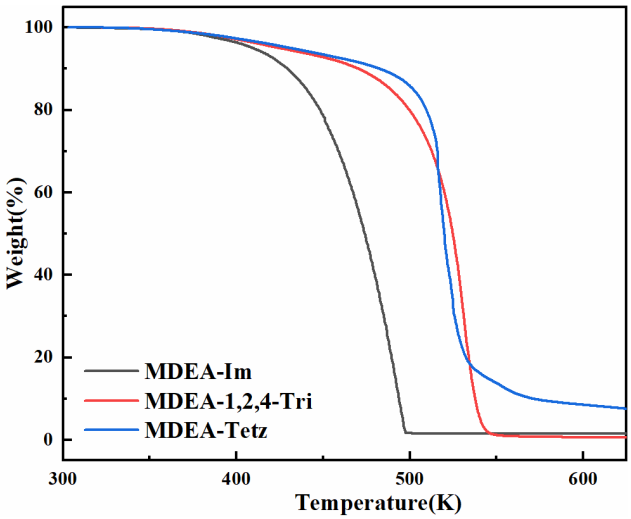

Figure S5. Thermal stability of DESs.

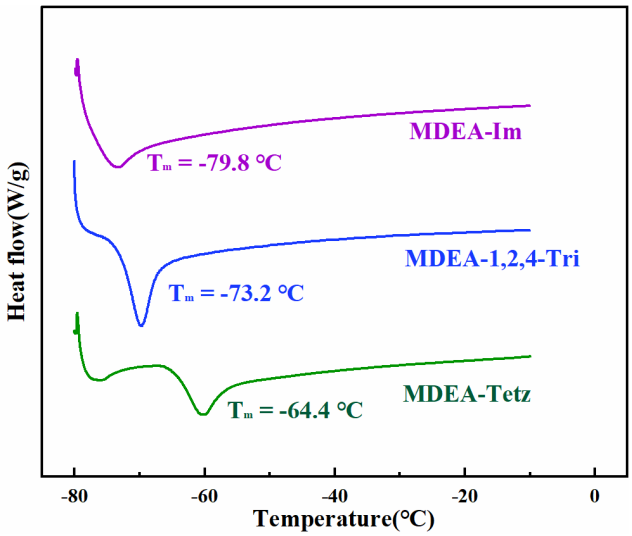

Figure S6. DSC curves and melting points of MDEA-Im/ 1,2,4-Tri/ Tetz.

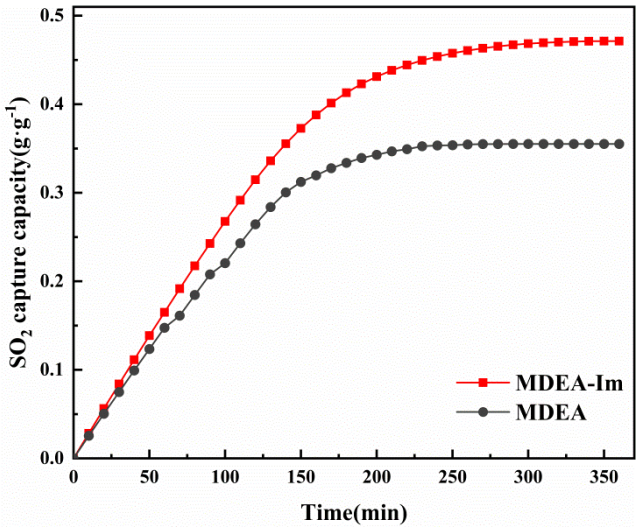

Figure S7. SO_2 capture capacity in MDEA and MDEA-Im at 293.2 K 2000 ppm

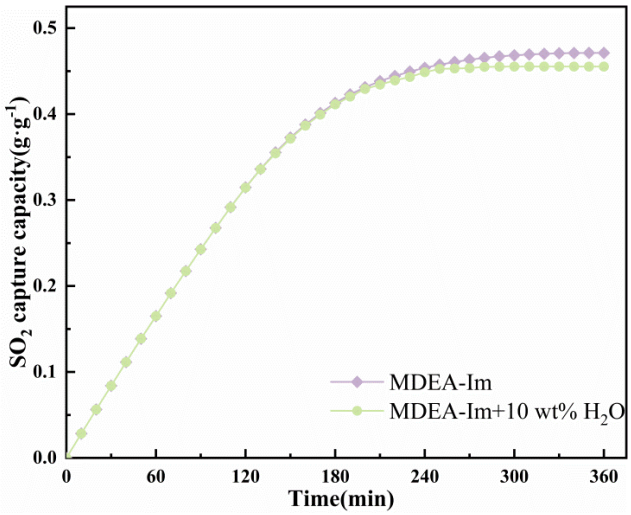

Figure S8. Effect of the mixture containing MDEA-Im and water on absorption

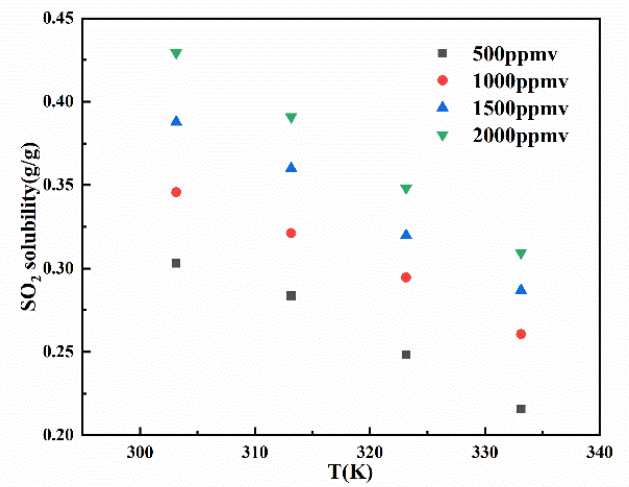

Figure S9. SO_2 capture capacity of MDEA-Im at different partial pressures and

temperature.

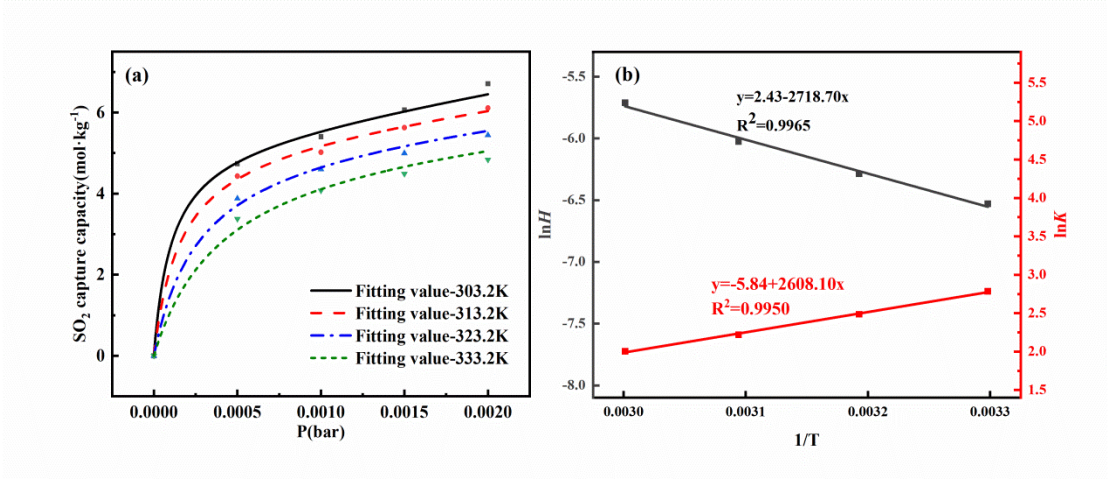

Figure S10. (a) Experimental measurements and fitting values of SO_2 in MDEA-Im. Symbols: measured in this study, ■303.2 K; ●313.2 K; ▲323.2 K; ▼333.2 K Curves: fitting values. (b) Dependence of ln*H* and ln*K* on 1/T.

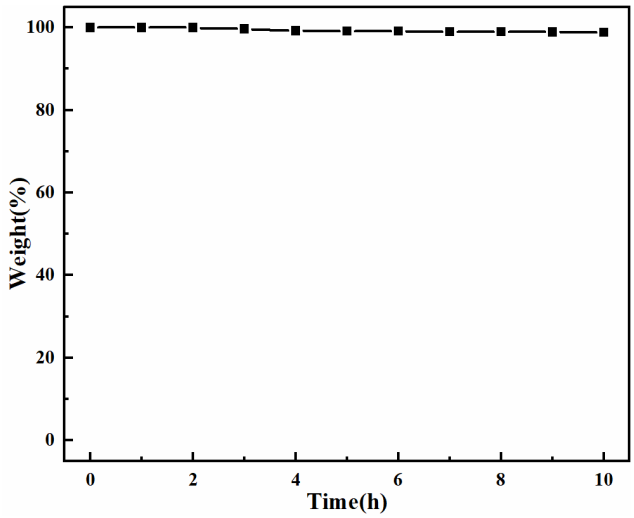

Figure S11. The weight loss of MDEA-Im (mass ratio = 1:1) at 363.2 K and N_2 flow rate of 1 L·min^{-1}.

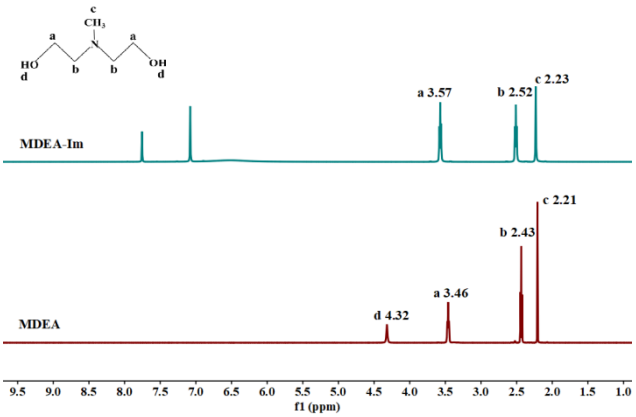

Figure S12. [1]H NMR spectroscopy of MDEA-Im and MDEA.

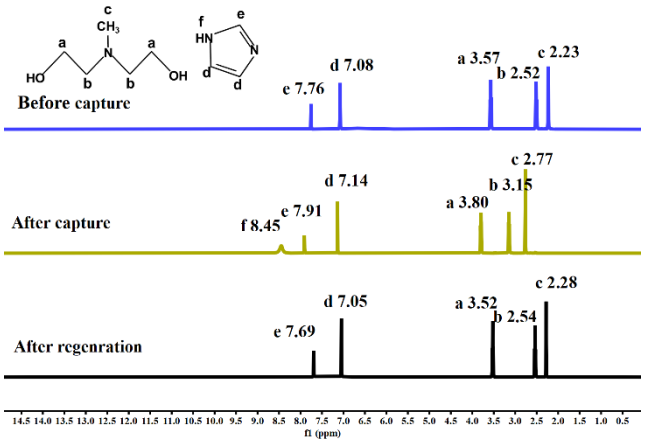

Figure S13. [1]H NMR spectroscopy of SO_2 captured by MDEA-Im(1:1) before and after SO_2 absorption and after regeneration.

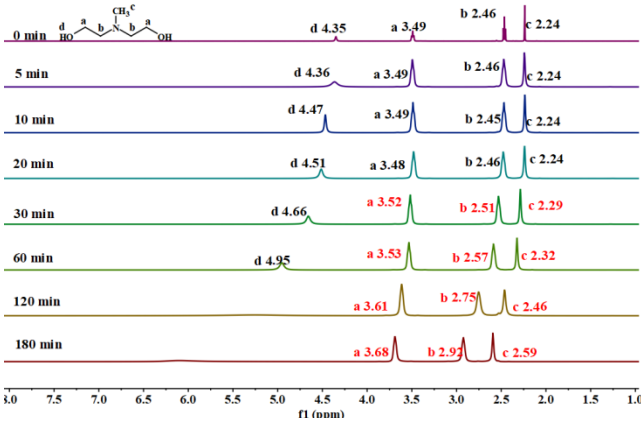

Figure S14. Time-dependent [1]H NMR spectroscopy of MDEA during SO_2 absorption process .

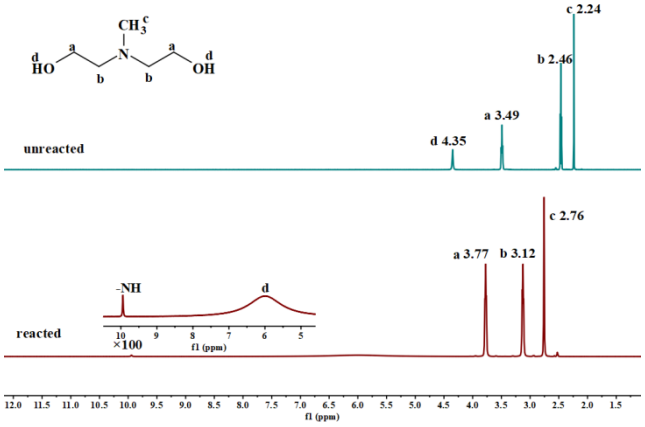

Figure S15. ^{1}H NMR spectroscopy of the interaction between MDEA and SO_2

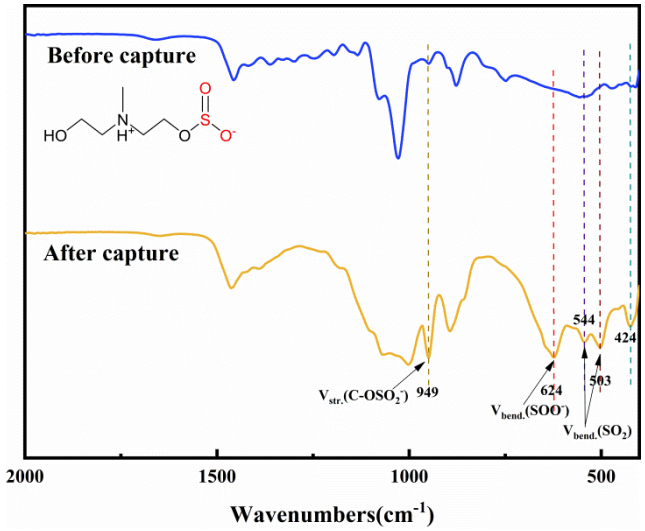

Figure S16. FT-IR spectroscopy of SO_2 captured by MDEA before and after SO_2 capture.

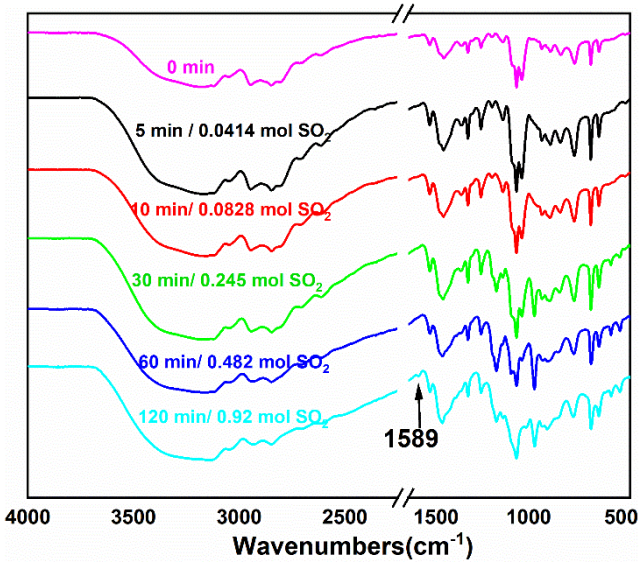

Figure S17. Time-dependent FT-IR spectroscopy of MDEA-Im during SO_2 absorption process.

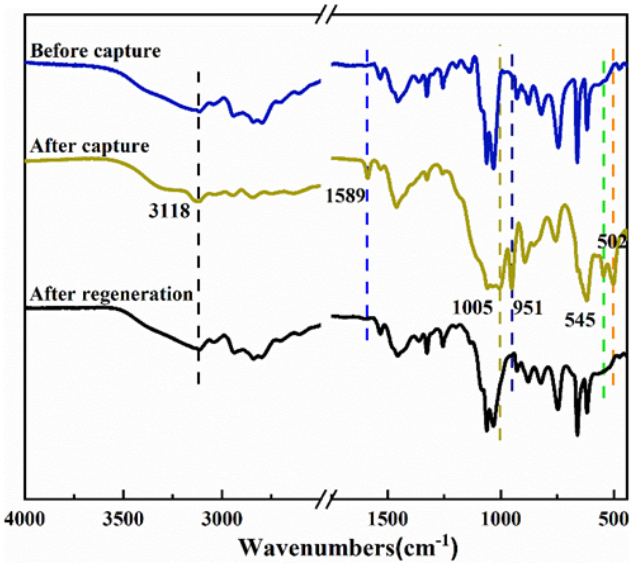

Figure S18. FT-IR spectroscopy of SO_2 captured by MDEA-Im before and after SO_2 capture and after regeneration.

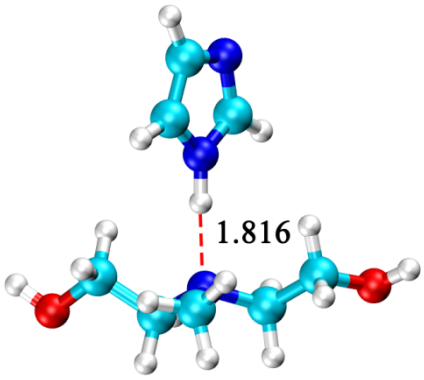

ΔH_B = -42.5 kJ·mol^{-1}

Figure S19. The interaction between between Im with MDEA. Optimized geometries of all species and the corresponding binding enthalpy changes are given. The white, cyan, blue, red, and yellow balls represent H, C, N, O, and S atoms, respectively.

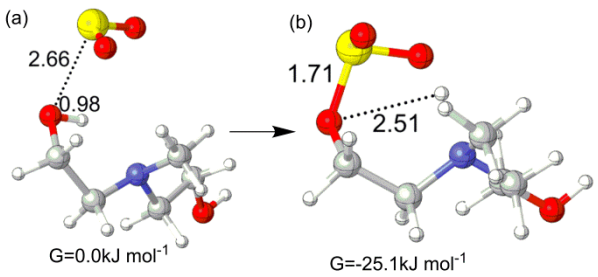

Figure S20. The optimized structure of the reaction between SO_2 and MDEA.The blue, red, and yellow balls represent N, O, and S atoms, respectively.

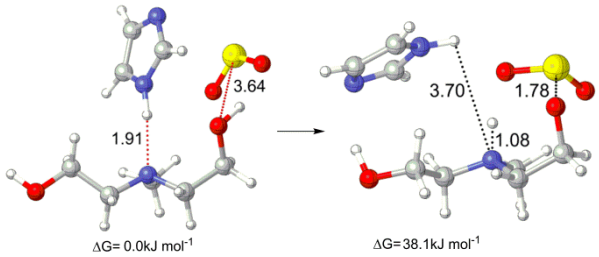

Figure S21. The interaction between SO_2 with MDEA-Im (molar ratio = 1:1). The blue, red, and yellow balls represent N, O, and S atoms, respectively.

Figure S22 The image of MDEA-Im(1:1) before and after SO_2 absorption.(left:before capture;right:after capture)

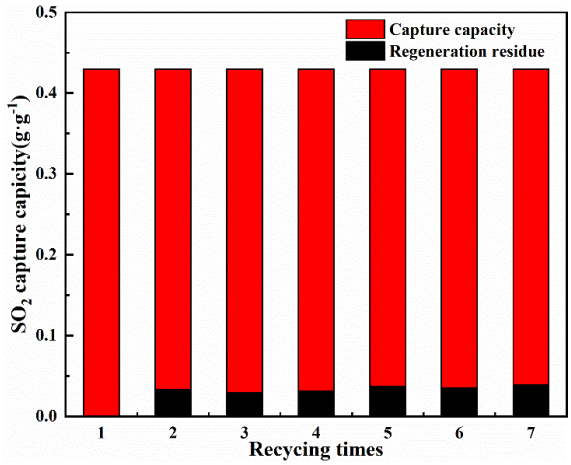

Figure S23. Recycle experiment of MDEA-Im: capture, 303.2 K and 2000 ppm; regeneration, 363.2 K and N_2 bubbling.

Table S1. Density of DESs at different temperatures.

Temperature(K)	Density (g·cm^{-3})		
	MDEA- Im	MDEA- 1,2,4-Tri	MDEA- Tetz
293.2	1.06722	1.11464[a]	1.20887[a]
303.2	1.05955	1.11031	1.20616
313.2	1.05226	1.1024	1.20059
323.2	1.04465	1.09503	1.19523
333.2	1.03708	1.08775	1.18967
R^2	0.999	0.998	0.999

[a] 298.2K

Table S2. Viscosity of DESs at different temperatures.

Temperature(K)	Viscosity(mPa·s)		
	MDEA- Im	MDEA- 1,2,4-Tri	MDEA- Tetz
293.2	273	220 [a]	1012 [a]

303.2	129	151	787
313.2	63	76	474
323.2	32	39	283
333.2	19	24	182
R^2	0.998	0.997	0.998

[a]298.2K

Table S3. Ionic conductivity of DESs(303.2 K)

DES	Ionic conductivity(mS/cm)
MDEA-Im	0.0112
MDEA-Tri	0.354
MDEA-Tetz	0.156

Table S4. Comparison of SO_2 capture capacity of ionic liquids (ILs) and DESs.

ILs/DESs[a]	T (K)	P (ppm)	Capture capacity ($g \cdot g^{-1}$)	ΔH_{Des} ($kJ \cdot mol^{-1}$)	Reference
MDEA-Im	293.2	2000	0.471	−44.71	This study
MDEA-1,2,4-Tri	293.2	2000	0.378	-	This study
MDEA-Tetz	293.2	2000	0.316	-	This study
EmimCl-PYD	293.2	2000	0.141	-	6
EmimCl-EG(1:1)	293.2	2000	0.047	−40.6	7
[TMEA][Im]	298.2	2000	0.321	−52.22	5
TEACl-Im(1:3)	293.2	2000	0.443	-	8
$[N_{2222}]$[Tetz]-EG(1:2)	293.2	2000	0.140	−52.7	9
$[E_3Eim_2]$[Im]	293.2	2000	0.267	-	10
4-CH_3-Im/BmimCl(2:1)	293.2	2000	0.354	-	11
2mEIP:8Tetz	293.2	2000	0.308	-	12

[TMG][MOAc]	293.2	6000	0.212	−54.62	13

[a]The full name and the composition of ILs/DESs were added in the Table S4.

Table S5. Capture capacity (mol·kg^{-1}) of MDEA-Im at different partial pressures and different temperatures.

T(K) / P(bar)	303.2	313.2	323.2	333.2
0.0005	4.737	4.431	3.88	3.372
0.001	5.403	5.019	4.603	4.073
0.0015	6.061	5.625	4.997	4.484
0.002	6.708	6.109	5.444	4.834

Table S6. The full name and the composition of ILs/DESs.

Namenclature	
Abbreviations	Full name
MDEA	N-Methyldiethanolamine
Im	Imidazole
1,2,4-Tri	1,2,4-Triazole
Tetz	Tetrazole
EmimCl	1-Ethyl-3-methylimidazolium chloride
PYD	2-Pyrrolidinone
EG	Ethylene glycol
[TMEA][Im]	Tris(3,6-dioxaheptyl) amine imidazole
TEACl	Tetraethylammonium chloride
[N_{2222}][Tetz]	Tetraethylammonium tetrazole
[E_3Eim_2][Im]$_2$	1,1′-(3,6,9-Trioxaundecane-1,11-diyl) bis (3-ethyl-1H-imidazolium-1-yl) imidazole
4-CH_3-Im	4-Methylimidazole
BmimCl	1-Butyl-3-methylimidazolium chloride
mEIP	N-methylated ethylene imine polymer
[TMG][MOAc]	1,1,3,3-Tetramethylguanidine methoxyacetate
EU	Ethylene urea

4-Op	4-Hydroxypyridine
MTPB	Methyltriphenyl phosphonium bromide
Bet	Betaine
ACC	Acetyl choline chloride
EPyBr	N-ethylpyridinium bromide
EPyCl	N-ethylpyridinium chloride
Mat	Matrine
MFA	N-methylformamide
$[BDMAEE][L]_2$	Bis(2-dimethylaminoethyl) ether dilactate

Table S7. Henry's constant and chemical equilibrium constant of SO_2 in MDEA-Im.

T(K)	303.2	313.2	323.2	333.2
H(bar)	0.00146	0.00186	0.00242	0.00331
K	16.208	12.037	9.213	7.428
R^2	0.997	0.998	0.996	0.996

Table S8. Variation of enthalpy and Gibbs value of SO_2 absorption in three sites of MDEA-Im ($kJ \cdot mol^{-1}$).

	Gaseous	
	Δ H	Δ G
MDEA–Im	-42.5	-5.9
MDEA + SO_2	-25.9	-25.1
MDEA–Im+ SO_2(a)	-61.6	-8.7
MDEA–Im+ SO_2(b)	-51.6	1.0
MDEA–Im+ SO_2(c)	-35.7	-1.2

Table S9: Cartesian coordinates for optimized geometries of all the species in gas phase.

MDEA–Im+ SO_2 (a)

C	0.08415300	-2.58633900	-0.33637800
H	-0.41064900	-2.42579300	0.62514100
H	0.00063800	-3.64856600	-0.59004100

C	1.55339100	-2.22548300	-0.27085100
H	1.95130400	-2.28954500	-1.28513600
H	2.08589200	-2.96508600	0.34940600
C	3.15670500	-0.44041700	-0.14114400
H	3.26044800	-0.59063500	-1.21896000
H	3.92142700	-1.05786200	0.35654400
C	3.43010200	1.02948100	0.16103500
H	3.47180300	1.21829600	1.23152000
H	2.64092500	1.65218700	-0.27123400
N	1.79753900	-0.86228200	0.22646700
O	-0.50963200	-1.77346200	-1.34915800
H	-1.47271100	-1.86167900	-1.27277000
O	4.71942900	1.41330300	-0.32401300
H	4.69401800	1.40859900	-1.29012100
C	1.60794800	-0.81412500	1.68231900
H	2.32690500	-1.46382700	2.20328000
H	1.73226800	0.20386100	2.04517500
H	0.59601100	-1.12579400	1.93186600
C	-0.34675100	2.11738300	0.52440700
C	-1.48847400	2.81226400	0.16527700
C	-1.22707100	1.26121100	-1.30191100
N	-0.19576100	1.13513800	-0.42515400
H	0.49249300	0.36185500	-0.38761100
H	0.33288600	2.23128200	1.35172900
H	-1.93279300	3.66065100	0.65986200
H	-1.33652100	0.61731300	-2.15815200
N	-2.04043400	2.27534100	-0.97564300
S	-3.17397100	-0.19679100	0.52383700
O	-3.29253000	-1.27857200	-0.49314500
O	-2.05729600	-0.30349800	1.49905400

MDEA–Im+ SO_2 (b)

C	2.88361400	-1.56562000	-0.09609400
H	2.28459000	-1.83765700	0.77999000
H	3.92405700	-1.44785300	0.21830200
C	2.33689000	-0.28663300	-0.71352700
H	1.48334600	-0.56166400	-1.33704600
H	3.09086600	0.17098900	-1.37131900
C	1.15776000	1.77515600	-0.36248000
H	0.43724800	1.33064100	-1.04880700
H	1.85003700	2.38256500	-0.96494700
C	0.40183500	2.66423900	0.62485900

H	1.05808700	3.39454800	1.09632200
H	-0.03585600	2.04097800	1.41205200
N	1.86230800	0.66519400	0.30125700
O	2.77702300	-2.56344600	-1.11797700
H	3.26145100	-3.35040300	-0.83577000
O	-0.60118400	3.42636100	-0.04106800
H	-1.31011200	2.81006300	-0.28174600
C	2.97086100	1.15897600	1.12439300
H	3.72758100	1.67161600	0.51248300
H	2.59507000	1.85503100	1.87168700
H	3.44401400	0.33069900	1.64927200
C	-1.40697900	-0.45055700	2.10066200
C	-2.42119000	-1.36950200	1.88687100
C	-0.84432100	-1.87422800	0.51603200
N	-0.40584000	-0.79461400	1.22460600
H	0.47589700	-0.26993200	1.04659500
H	-1.31800000	0.37950500	2.78105100
H	-3.37452500	-1.43100300	2.38572600
H	-0.23733200	-2.36891300	-0.22704700
N	-2.07176000	-2.25495200	0.89651700
S	-2.29564000	-0.14408300	-1.45691100
O	-2.42433700	0.97270200	-0.47778300
O	-1.10024900	-0.13739900	-2.34031900

MDEA–Im+ SO_2 (c)

C	-2.05415300	2.45596300	-0.31880600
H	-0.98356300	2.27956200	-0.45160400
H	-2.24519800	2.61833600	0.74687100
C	-2.83875500	1.26155000	-0.83665200
H	-2.49933600	1.04003900	-1.84886000
H	-3.90399300	1.52422900	-0.89459400
C	-2.82796900	-1.15259600	-0.79246600
H	-2.14978400	-1.11543900	-1.64655800
H	-3.85644600	-1.20872200	-1.17958900
C	-2.51031600	-2.42026000	-0.01642900
H	-3.26719000	-2.62081100	0.74634500
H	-1.53510400	-2.32251800	0.47086500
N	-2.62666400	0.06860900	0.00380200
O	-2.49559700	3.57824900	-1.08780800
H	-1.88986600	4.31489600	-0.93515200
O	-2.49762800	-3.46490300	-0.99409300
H	-2.33733100	-4.30559700	-0.54645600

C	-3.53146500	0.09066700	1.16185400
H	-4.57265400	-0.08817200	0.85956800
H	-3.23697200	-0.66816300	1.88555000
H	-3.47593400	1.06109300	1.65134000
C	0.48371800	0.25127400	2.27143900
C	1.85274000	0.05694900	2.25645700
C	1.14774400	-0.36115400	0.25999600
N	0.05430000	-0.01806200	0.99337200
H	-0.92274300	0.03279400	0.63929800
H	-0.19181400	0.55312200	3.05411100
H	2.55471900	0.17228900	3.06556600
H	1.11050000	-0.60944500	-0.78913400
N	2.25742100	-0.32643500	0.99862200
S	4.39332200	-0.31372900	-0.58677700
O	3.51402600	-0.53433100	-1.76253700
O	4.85230900	1.07086300	-0.32081900

MDEA+SO_2(a)

C	-2.888843	-1.03087	-0.08505
H	-2.265353	-1.49251	-0.85768
H	-2.746999	-1.59089	0.843562
O	-4.265195	-0.9989	-0.45441
H	-4.570499	-1.91047	-0.52143
C	-2.471741	0.420119	0.07632
H	-3.030503	0.869024	0.910425
H	-2.767055	0.939085	-0.83589
N	-1.026225	0.565524	0.243534
C	-0.57568	0.043764	1.536191
H	0.495047	0.192741	1.645623
H	-1.091047	0.536966	2.371639
H	-0.755297	-1.02663	1.589628
C	-0.588476	1.951596	0.053207
H	-0.764362	2.58187	0.936274
H	-1.161907	2.364661	-0.7773
C	0.89087	1.946862	-0.32921
H	1.173466	2.904576	-0.76695
H	1.526199	1.774557	0.544743
O	1.105471	0.922951	-1.30032
H	0.35883	0.309337	-1.12095
S	2.770102	-0.88527	-0.28619
O	1.678579	-1.88245	-0.24626
O	3.014225	-0.07105	0.926464

MDEA+SO_2(b)

C	2.582983	0.782732	-0.33839
H	2.35934	0.729232	-1.40757
H	2.014741	1.63248	0.066134
O	3.987599	0.973407	-0.24633
H	4.194807	1.230822	0.661473
C	2.166747	-0.509	0.379765
H	2.45308	-0.41607	1.433433
H	2.733727	-1.35737	-0.03368
N	0.710617	-0.75479	0.335061
C	0.269591	-1.65691	1.41469
H	-0.82073	-1.68513	1.444148
H	0.670483	-2.6739	1.288299
H	0.612258	-1.25869	2.372632
C	0.280376	-1.23813	-0.99567
H	0.580029	-2.29117	-1.13021
H	0.796023	-0.64909	-1.75667
C	-1.2215	-1.12069	-1.26191
H	-1.43423	-1.56144	-2.24071
H	-1.81538	-1.65818	-0.51567
O	-1.65551	0.244077	-1.35248
H	0.25114	0.0788	0.491479
S	-2.13059	1.007357	0.100378
O	-0.66886	1.475106	0.618184
O	-2.61842	-0.0752	0.990598

References

1. M.J, Frisch; G.W, Trucks; H.B, Schlegel; G.E, Scuseria; M.A, Robb; J.R, Cheeseman; G, Scalmani; V, Barone; B, Mennucci; G.A, Petersson; et al. Gaussian 09, Revision D.01; Gaussian Inc.: Wallingford, CT, USA, 2013
2. Humphrey, W. Dalke, A. Schulten, K, *Journal of Molecular Graphics*, 1996,**14**,33-38.
3. C. Cheng, J. Li, J. Cao, J. Guo and W. Cen, *Journal of Hazardous Materials*, 2021, **408**, 124462.
4. K. Huang, Y.-L. Chen, X.-M. Zhang, S. Xia, Y.-T. Wu and X.-B. Hu, *Chemical Engineering Journal*, 2014, **237**, 478-486.
5. P. Liu, K. Cai, X. Zhang and T. Zhao, *AIChE Journal*, 2022, **68**, e17596.
6. P. Li, X. Wang, T. Zhao, C. Yang, X. Wang and F. Liu, *Chemical Engineering Journal*, 2021, **422**, 129114.
7. D. Yang, Y. Han, H. Qi, Y. Wang and S. Dai, *ACS Sustainable Chemistry & Engineering*, 2017, **5**, 6382-6386.
8. P. Zhang, G. Xu, M. Shi, Z. Wang, Z. Tu, X. Hu, X. Zhang and Y. Wu, *Separation and*

Purification Technology, 2022, **286**, 120489.

9. G. Cui, D. Yang and H. Qi, *Industrial & Engineering Chemistry Research*, 2021, **60**, 4536-4541.
10. D. Li, Y. Kang, J. Li, Z. Wang, Z. Yan and K. Sheng, *Separation and Purification Technology*, 2020, **240**, 116572.
11. S. Hou, C. Zhang, B. Jiang, H. Zhang, L. Zhang, N. Yang, N. Zhang, X. Xiao and X. Tantai, *ACS Sustainable Chemistry & Engineering*, 2020, **8**, 16241-16251.
12. D. Li and Y. Kang, *Journal of Hazardous Materials*, 2021, **404**, 124101.
13. Z. Geng, S. Ma, Y. Li, C. Peng, B. Jiang, P. Liu and Y. Xu, *Industrial & Engineering Chemistry Research*, 2022, **61**, 4493-4503.